Journal of Alloys and Compounds 883 (2021) 160869

Contents lists available at ScienceDirect

Journal of Alloys and Compounds

journal homepage: www.elsevier.com/locate/jalcom

Equiatomic quaternary Heusler compounds TiVFeZ (Z=Al, Si, Ge): Half-metallic ferromagnetic materials

A. Gencer[a], O. Surucu[b], D. Usanmaz[c], R. Khenata[d], A. Candan[e], G. Surucu[f,g,*]

[a] Department of Physics, Karamanoglu Mehmetbey University, Karaman 70100, Turkey
[b] Department of Electrical and Electronics Engineering, Atilim University, Ankara 06836, Turkey
[c] Department of Physical Sciences, Arkansas Tech University, Russelville, AR 72801, USA
[d] Laboratoire de Physique Quantique de la Matiére et de Modélisation Mathématique (LPQ3M), Université de Mascara, 29000 Mascara, Algeria
[e] Department of Machinery and Metal Technology, Ahi Evran University, Kirsehir 40100, Turkey
[f] Department of Physics, Middle East Technical University, Ankara 06800, Turkey
[g] Department of Electric and Energy, Ahi Evran University, Kirsehir 40100, Turkey

ARTICLE INFO

Article history:
Received 4 April 2021
Received in revised form 30 May 2021
Accepted 16 June 2021
Available online 24 June 2021

Keywords:
Equiatomic quaternary Heusler compounds
Density functional theory
Ferromagnetic
Half-metallic
Electronic properties
Magnetic properties

ABSTRACT

Equiatomic quaternary Heusler compounds (EQHCs) are very promising materials for spintronic applications due to their excellent electronic and magnetic properties. In this study, structural, electronic, magnetic, mechanic, and dynamic properties of TiVFeZ (Z=Al, Si, Ge) EQHCs are investigated. Three nonequivalent structural configurations of α, β, and γ type structures are considered. The γ is defined as the most stable phase for all these compounds and has a half-metallic character. The predicted Curie temperatures of TiVFeAl, TiVFeSi, and TiVFeGe compounds are about 488 K, 256 K, and 306 K, respectively. We also show that TiVFeZ (Z=Al, Si, Ge) have thermodynamic, dynamic, and mechanical stabilities. The presented results reveal that these compounds are potential materials for spintronics applications.

1. Introduction

Spintronics is very promising for next-generation information technology; it uses the electrons' spin to transmit and process information. Using spins instead of the electrons' charge enables increased data processing speed, less heat dissipation, and low power consumption. Half-metallic materials with a perfect spin-polarization at the Fermi level are the most suitable for spintronic applications. Several material classes such as diluted magnetic semiconductors [1,2], transition metal oxides [3,4], double-perovskites [5], and Heusler compounds [6] have half-metallic character. Searching for new half-metallic ferromagnetic and half-metallic antiferromagnetic materials within these classes is essential to increase the spintronic devices' performance. Among these materials, Heusler compounds — full-Heusler, half-Heusler, and equiatomic quaternary Heusler compounds [7–9] — have potential due to their high Curie temperature (T_C) and tunable magnetic and electronic properties.

Full Heusler compounds – X_2YZ, where X and Y are transition metals and Z is a main-group/sp element [10] – have a cubic $L2_1$ structure (space group, $Fm\bar{3}m$ #225), which is formed by four interpenetrating fcc sublattices. In quaternary Heusler compounds ($XX'YZ$), each of these sublattices is occupied by different atoms, and the structure has different symmetry (space group $F\bar{4}\,3m$ #216). The structure is named as Y-type (LiMgPdSn prototype) [11,12] and X, X', Y, and Z atoms occupy the $4a$(0, 0, 0), $4b$(1/4, 1/4, 1/4), $4c$(1/2, 1/2, 1/2), and $4d$(3/4, 3/4, 3/4) Wyckoff positions, respectively.

Since quaternary Heusler compounds have four distinct atoms with a 1:1:1:1 stoichiometry [13], they are named equiatomic quaternary Heusler compounds (EQHCs). The interest for the EQHCs has been increasing due to their advanced properties: half metallicity with high T_C and large magnetization [14–16], good thermoelectric properties [17,18], and topological character [19,20]. They also have enhanced properties compared to pseudo-ternary compounds [21]. Especially, Fe containing EQHCs have good properties for spintronic applications. Known highest T_C values, 867 K, 833 K, and 866 K, were obtained for CoRuFeSi [22], CoRuFeGe [22], and CoFeCrGe [15], respectively. CoFeMnSi and CoFeMnGe materials also have high T_C

* Corresponding author at: Department of Physics, Middle East Technical University, Ankara 06800, Turkey.
E-mail address: info@gokhansurucu.com (G. Surucu).

https://doi.org/10.1016/j.jallcom.2021.160869
0925-8388/

values and interesting magnetic behavior: the magnetic moment at Fe sites changed with the number of valence electrons, and also the sign changed by increasing the valence electron from 27 to 28 [23]. Calculations reveal that CoFeTiSi, CoFeTiAs, and CoFeVSb are ferromagnetic materials and have 0.31, 0.18 and 0.17 eV half-metallic gap, respectively [24] and CoFeMnSi is a spin gapless semiconductor [16]. It is also reported that increasing the Z atom's size causes the decreasing bandgap in the CoFeTiZ (Z=Si, Ge, Sn) systems [25].

All these studies show that obtaining EQHCs with advanced properties is possible, and further research on the new EQHCs is essential for spintronics applications. In this study, the thermodynamically stable phase of TiVFeZ (Z = Al, Si, Ge) EQHCs is defined by considering three nonequivalent structural configurations (α, β, and γ) of Y-type structure [12,26]. In order to identify the most stable magnetic ordering, three magnetic types — anti-ferromagnetic (AFM), ferromagnetic (FM), and paramagnetic (PM) — are considered, and the Curie temperatures for these compounds are determined. Spin-polarized electronic band structure and density of states (DOS) calculations enable the electronic characterization. Mechanical and dynamic stabilities — crucial for technological applications — are investigated.

2. Computational method

In this study, Density Functional Theory (DFT)-based calculations are performed using the Vienna Ab-initio Simulation Package (VASP) [27,28] for TiVFeZ (Z = Al, Si, Ge) compounds. The Perdew-Burke-Ernzerhof (PBE) functional [29] within the Generalized Gradient Approximation (GGA) is employed for the exchange-correlation functional of the electron-electron interactions. In addition, the Projector Augmented Wave (PAW) method [30,31] is applied for the interactions between the electrons and the ions. Geometrical optimizations are performed up to an energy convergence of 10^{-11} eV/unit-cell and force convergence as 10^{-10} eV/Å. The 500 eV cut-off energy TiVFeSi and TiVFeGe, and 550 eV cut-off energy for TiVFeAl for the planewaves are selected. The **k**-points in the irreducible Brillouin zone are sampled using a Γ-centered scheme [32] with 16×16×16 **k**-points. Also, the valence electron configurations are taken as $3d^3 4s^1$, $3p^6 3d^4 4s^1$, $3p^6 4d^7 4s^1$, $3s^2 3p^1$, $3s^2 3p^2$ and $4s^2 4p^2$ for Ti, V, Fe, Al, Si, and Ge atoms, respectively. The elastic constants of these compounds are obtained with the stress-strain method using VASP [27,28,33]. Bader charges are analyzed by using the Bader Charge Analysis Code [34]. The dynamic properties of the TiVFeZ (Z = Al, Si, Ge) compounds are calculated using the PHONON software [35] to calculate the phonon branches with the Direct method [36]. Furthermore, the spin-orbit coupling (SOC) is considered to couple the spin orientation to the crystal structure [37].

Table 1
The calculated lattice constants (a in Å), formation energies ΔE_f in eV/atom), total magnetic moments (M_t in μ_B), and partial magnetic moments of atoms (M_{Ti}, M_V, and M_{Fe} in μ_B) for TiVFeZ (Z = Al, Si and Ge) compounds in the α, β, and γ phases.

Compound	Phase	a	ΔE_f	M_t	M_{Ti}	M_V	M_{Fe}
TiVFeAl	α	6.047	0.015	0.901	0.145	0.915	−0.166
	β	6.018	−0.048	1.710	0.945	0.663	0.101
	γ	6.034	−0.122	1.758	0.351	1.855	−0.447
TiVFeSi	α	5.982	−0.211	2.316	−0.035	0.327	1.983
	β	5.902	−0.159	1.964	0.921	0.387	0.657
	γ	5.903	−0.324	2.738	0.137	1.952	0.660
TiVFeGe	α	6.064	−0.087	2.563	−0.028	0.541	2.010
	β	5.998	0.000	2.175	0.947	0.336	0.905
	γ	5.994	−0.152	2.719	0.097	1.979	0.665

3. Results and discussions

The EQHCs have a cubic structure with space group $F\bar{4}3m$, #216 [11,12], and the structure is named Y-type: the prototype is LiMgPdSn and has fcc primitive cell where atoms occupy the 4*a*, 4*b*, 4*c*, and 4*d* Wyckoff positions. By considering all possible atomic configurations, this prototype has only three nonequivalent structures [11,12]. In this study, the structures are referred to as α, β, and γ (Fig. 1), where the main group element occupy the 4*d* site while the 4*a*, 4*b*, and 4*c* positions are interchangeable to the transition metal elements (Fig. 1).

The lattice parameters, formation energies, and magnetic moments of fully optimized structures are presented in Table 1. Our calculated lattice parameters for TiVFeAl and TiVFeSi are consistent with previously reported 6.04 Å and 5.91 Å values, respectively [12]; however, there are no reported results for TiVFeGe.

Formation energies are calculated by using

$$\Delta E_f = E^{TiVFeZ} - E^{Ti} - E^{V} - E^{Fe} - E^{Z}, \quad (1)$$

where E^{TiVFeZ} is the total energy of the corresponding phase, and E^{Ti}, E^{V}, E^{Fe}, and E^{Z} are the ground state energies of the Ti, V, Fe, and Z (Si, Ge, Al) atoms. Calculations reveal that the γ phase is the most stable phase for all three systems: TiVFeAl, TiVFeSi, and TiVFeGe (Table 1 and Fig. S1).

Three magnetic types – AFM, FM, and PM – are considered to define the magnetic character of the γ phase, and FM arrangement is defined as most stable type for TiVFeZ compounds. The energy-volume graphs are presented in Supplementary file (Fig. S2). Furthermore, Fig. S3 shows the energy and enthalpy change with respect to pressure for the FM type of the γ phases of TiVFeZ compounds. As can be seen from the figure, these compounds have the lowest

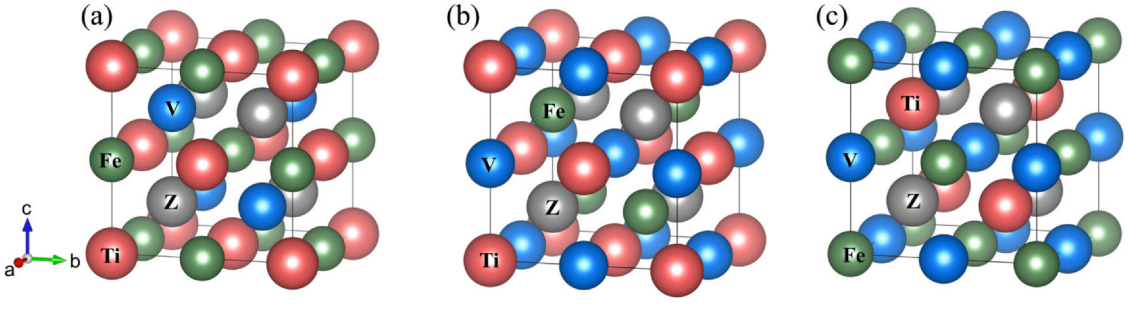

Fig. 1. The crystal structures of (a) α, (b) β, and (c) γ phases of TiVFeZ (Z = Al, Si, Ge).

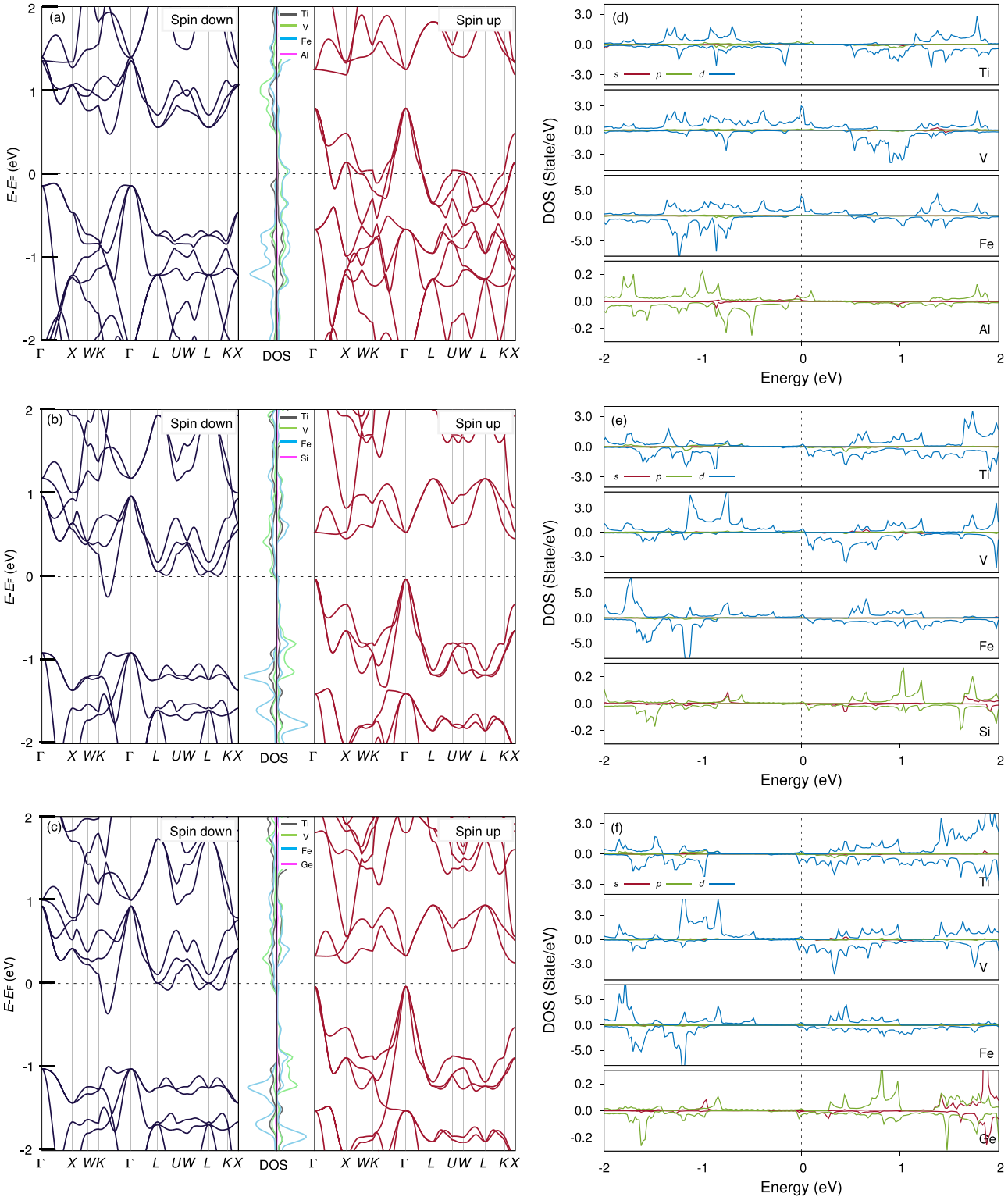

Fig. 2. Band structures for spin up and spin down channels with density of states for (a) TiVFeAl, (b) TiVFeSi and (c) TiVFeGe and detailed partial density of states (PDOS) for (d) TiVFeAl, (e) TiVFeSi and (f) TiVFeGe.

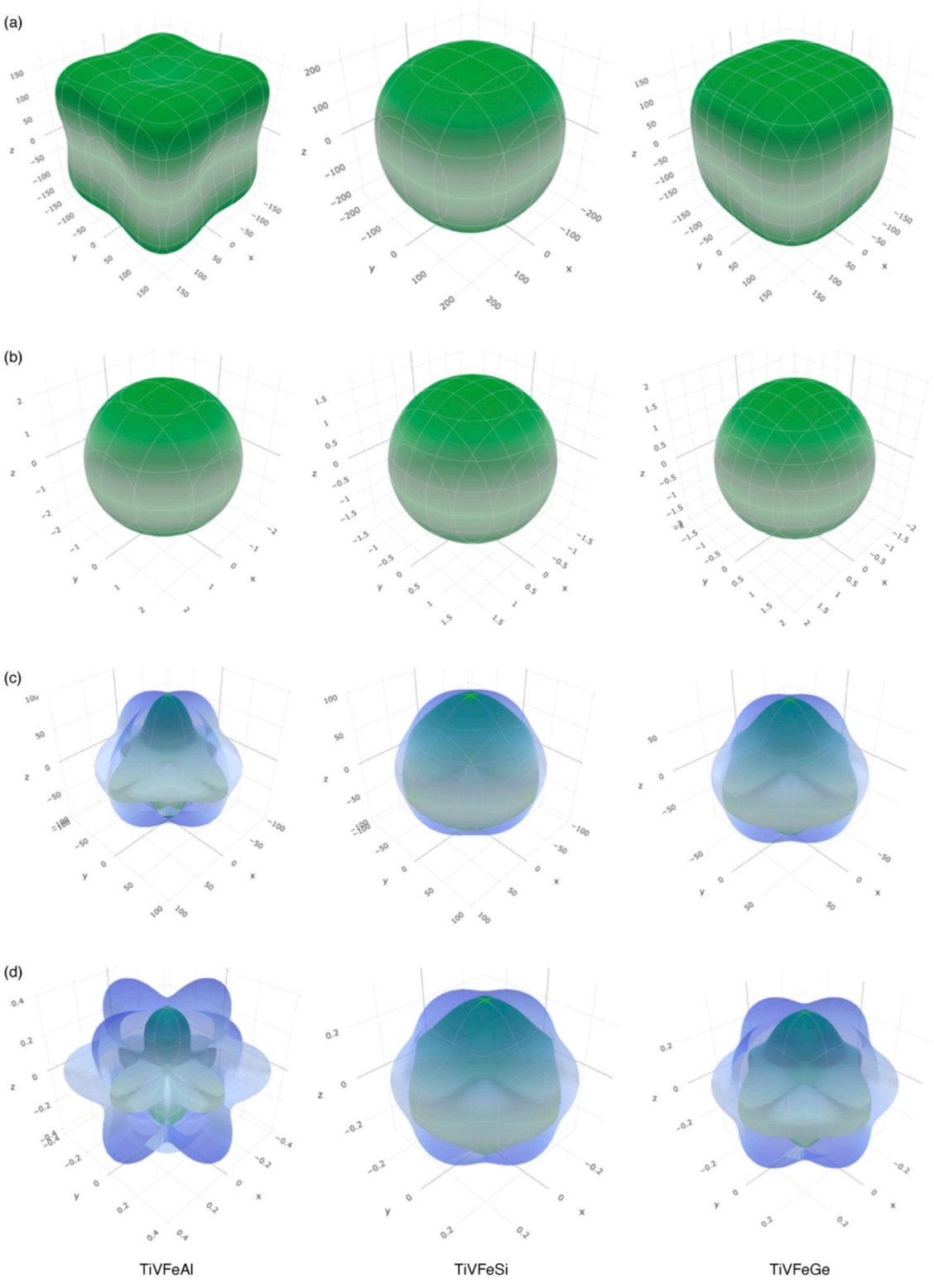

Fig. 3. 3D representation of (a) Young's modulus, (b) linear compressibility, (c) shear modulus and (d) Poisson's ratio for TiVFeZ (Z = Al, Si, Ge) compounds.

Table 2
The elastic constants (C_{ij}, in GPa), and Cauchy pressures (C_p, in GPa) for TiVFeZ (Z = Al, Si and Ge) compounds in the α, β, and γ phases.

Compound	Phase	C_{11}	C_{12}	C_{44}	C_p
TiVFeAl	α	117.38	147.91	77.76	Unstable mechanically
	β	229.48	146.45	57.28	89.17
	γ	212.40	112.30	97.00	15.30
TiVFeSi	α	139.30	208.14	73.08	Unstable mechanically
	β	214.17	149.78	53.73	96.05
	γ	299.90	129.60	98.40	31.20
TiVFeGe	α	122.60	181.57	71.79	Unstable mechanically
	β	189.15	140.87	92.47	48.40
	γ	264.00	128.30	91.40	36.90

energy at zero pressure; moreover, the enthalpy value becomes positive above 27 GPa for TiVFeAl and 32 GPa for TiVFeGe, whereas TiVFeSi has negative enthalpy values up to 40 GPa. Therefore, TiVFeAl is stable up to a maximum of 27 GPa, TiVFeGe is stable up to a maximum of 32 GPa, and TiVFeSi is stable up to 40 GPa within the limits of the present study which could be further expanded. In addition, the Curie temperature (T_C) is determined using the mean field approximation $2\Delta E = 3k_BT_C$ [38]. In this equation, ΔE is the energy difference between the antiferromagnetic and ferromagnetic phases, and k_B is the Boltzmann constant. Using the calculated energies for AFM and FM phases, the Curie temperatures per atom are predicted as about 488 K, 256 K, and 306 K for TiVFeAl, TiVFeSi, and TiVFeGe, respectively.

The γ phase also has the highest total magnetic moments among the three phases (Table 1) Interestingly a large contribution comes from the V atom rather than the magnetic element Fe. Similar behavior is observed in various EQHCs [39]. It is important to note that the sign of the magnetic moment at the Fe site is changed with increasing valence electron number in the system; in TiVFeAl, the Fe atom's magnetic moment is antiparallel to Ti and V atoms [23].

The electronic properties of the FM γ phases for TiVFeZ compounds are investigated. The spin-polarized electronic band structure and density of states (DOS) calculations (Fig. 2) reveal that these compounds are half-metallic. TiVFeAl has a metallic nature in the spin-up channel and a clear band gap (0.59 eV - indirect) in the spin-down channel. In contrast, TiVFeSi and TiVFeGe have a metallic character in the spin-down channels and 0.49 eV and 0.28 eV indirect band gaps from Γ to X in the spin-up channels, respectively. Fig. 3(d)-(e) shows the detailed partial density of states (PDOS) to analyze the orbital contributions around the Fermi level (E_F). For TiVFeAl, the main contribution to DOS around the E_F comes from the (spin-up) d orbitals of the Ti, V, and Fe atoms. However, the origin of the metallic character in TiVFeSi and TiVFeGe is the (spin-down) d orbitals of the Ti, V, and Fe atoms. In general, the s and p states of these atoms do not have a significant effect on the PDOS. For the Z atoms, the p states of Al atoms are dominant both above and below the Fermi level, while the p states of Si and Ge atoms are dominant below this level, and the s states of these atoms contribute more in the energy range between 1.5 and 2.0 eV. In addition to these contributions to the PDOS, the Bader charge relations could be determined as listed in Table S1.

In addition to these detailed electronic properties, the spin-orbit coupling is considered for these compounds and the magnetization direction is taken along the [2 2 2] direction. The results for the spin-orbit coupling studies are given in Fig. S4. As can be seen from the figures, the spin-orbit coupling results with the metallic nature for these compounds. This feature is due to inability to visualize the spin-up and spin-down orientations for spin-orbit coupling calculations.

The elastic constants (C_{ij}) calculation allows us to determine the mechanical stability and the mechanical characteristics of the material, such as brittleness and hardness. There are 21 independent elastic constants in general; for the cubic systems, this number reduces to 3 constants as C_{11}, C_{12}, and C_{44} due to the symmetry. The calculated elastic constants and the Cauchy pressures for α, β, and γ phases are listed in Table 2. Mechanically stable materials should satisfy the Born stability criteria [40]:

$$C_{11} - C_{12} > 0$$
$$C_{11} + 2C_{12} > 0$$
$$C_{11} > 0 C_{44} > 0 \quad (2)$$

and our calculations reveal that only β and γ phases are mechanically stable for TiVFeZ. The Cauchy pressure is the difference between the C_{12} and C_{44}, and the negative value indicates the brittleness while the positive indicates a ductile nature. The γ phases of the TiVFeZ have a positive value for the Cauchy pressure that represents ductility.

The elastic constants are also used to determine the mechanical properties, such as bulk modulus (B), shear modulus (G), Young's modulus (E), and Poisson's ratio (ν). Among these three systems, TiVFeZ (Z = Al, Si, and Ge), the highest bulk, shear, and Young's moduli are obtained for TiVFeSi (Table 3). Compare to TiVFeAl and TiVFeGe, TiVFeSi is more resistant to compression and shearing deformation, and also it is more stiffer. The material's bonding nature is examined using the Poisson's ratio — the transverse strain to axial strain ratio. The 0.25 value for the Poisson's ratio implies that the material has dominantly ionic bonding, while the 0.1 value represents the covalent bonding [42]. Our calculated values are around 0.28; these materials have mainly ionic bonding. The G/B ratio can help obtain information about the bonding character: the 0.6 value indicates ionic bonding while 1.1 indicates covalent bonding [41]. Calculated G/B values (~ 0.5) show that TiVFeZ compounds have an

Table 3
The bulk modulus (B in GPa), shear modulus (G in GPa), Young's modulus (E in GPa), Poisson's ratio ν, G/B ratio, B/G ratio, and linear compressibility (β), for TiVFeZ (Z = Al, Si and Ge) compounds.

Compound	B	G	E	ν	G/B	B/G	E_{min}	E_{max}	β_{min}	β_{max}	G_{min}	G_{max}	ν_{min}	ν_{max}
TiVFeAl	145.6	74.3	190.4	0.282	0.510	1.959	134.72	238.14	2.29	2.29	50.05	97.00	0.03	0.51
TiVFeSi	186.3	92.8	238.7	0.286	0.498	2.007	221.69	251.02	1.79	1.79	85.15	98.40	0.23	0.33
TiVFeGe	173.5	81.0	210.2	0.298	0.466	2.141	180.08	233.25	1.92	1.92	67.85	91.40	0.19	0.39

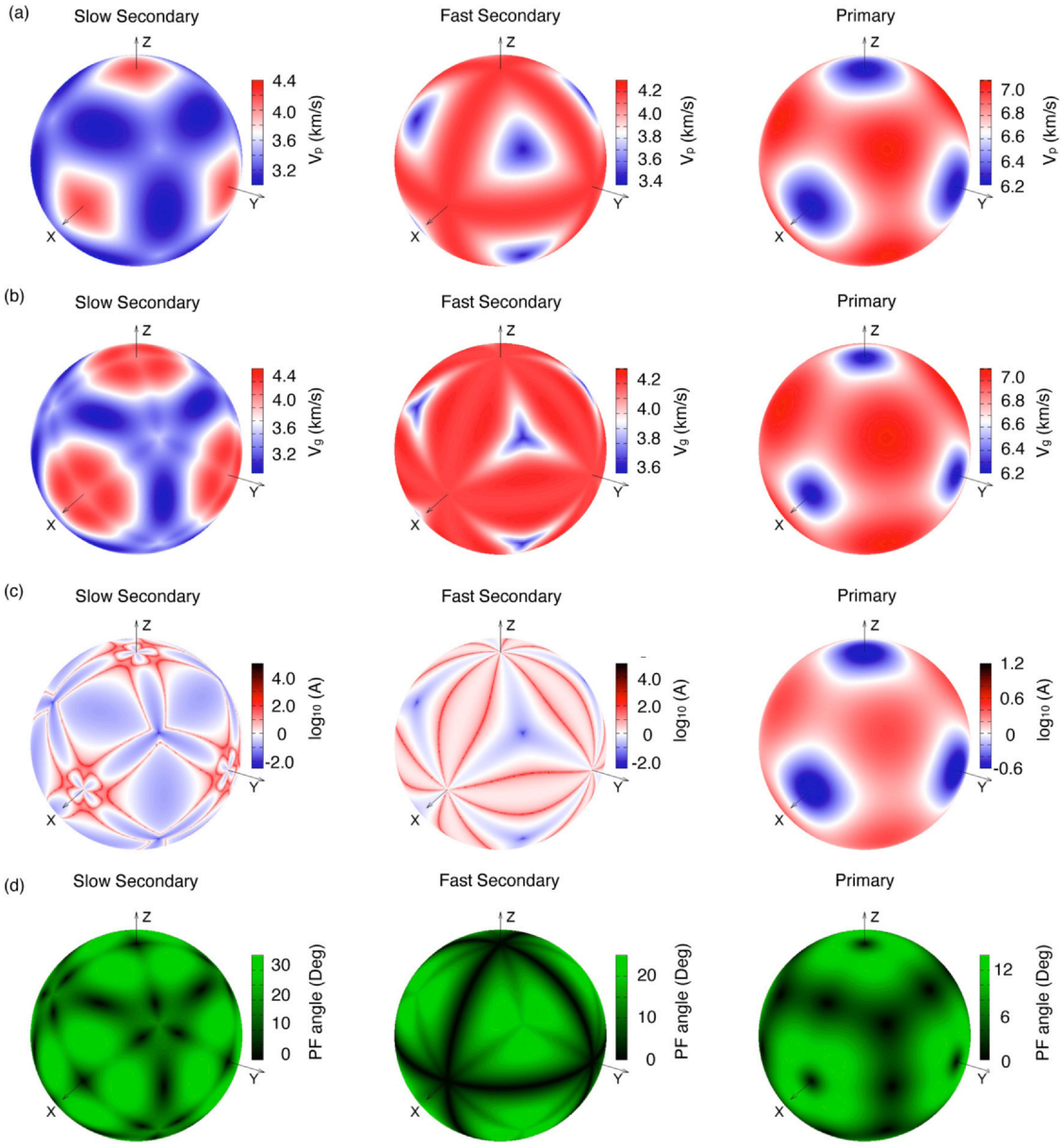

Fig. 4. (a) Phase velocity, (b) group velocity, (c) enhancement factor and (d) power flow angle for TiVFeAl.

ionic bonding character. The *B/G* ratio is useful to discuss the brittleness or ductility of a material, and 1.75 is the threshold value between brittleness and ductility [42]. The TiVFeZ compounds are ductile with *B/G* ratios higher than 1.75; this is consistent with Cauchy pressure.

The visualization of the mechanical properties in 3D provides information about the anisotropic properties, crucial for the industrial applications concerning micro-cracks and dislocations. Fig. 3 presents the direction-dependent Young's modulus, linear compressibility, shear modulus, and Poisson's ratio for TiVFeZ in 3D. The spherical and distorted shapes indicate isotropy and anisotropy, respectively. Linear compressibility is isotropic, while Young's modulus, shear modulus, and Poisson's ratio are anisotropic. Also, the blue and green indicate the maximum and minimum values as listed in Table 3.

Additionally, soundwave velocities are found with the Christoffel tool [43] after calculating the elastic constants and density of the compounds to solve the respective equation [44], and this relation is

presented in Eq. (3) with two soundwave velocities, longitudinal and transverse.

$$C_{11} = \rho(V_{LA}[100])^2$$
$$C_{44} = \rho(V_{TA}[110]_{<001>})^2 \quad (3)$$

The longitudinal wave velocity along the [100] direction is proportional to C_{11}, and the transverse one along the [110] direction is proportional to C_{44}. For these compounds, C_{11} values are higher than C_{44}, so the longitudinal wave velocity is higher than the transverse wave velocity. Fig. 4 shows the phase velocity, group velocity, enhancement factor, and phase polarization angle for TiVFeAl. Figures for TiVFeSi and TiVFeGe are presented in Supplementary file (Figs. S5 and S6). The slow secondary and the fast secondary spheres correspond to transverse wave velocities, while the primary sphere corresponds to the longitudinal wave velocity. The phase wave velocity is fast along *x*, *y*, and *z* directions for the slow secondary and fast secondary phase; it has lower values in the same directions for the primary phase. A similar behavior could be seen in Fig. 4(b) for the group wave velocity. The enhancement factor is the ratio of the group wave velocity's to the phase wave velocity's direction: it has higher values along *x*, *y*, and *z* directions for the slow secondary and fast secondary phases. Conversely, it has lower values for the primary phase. The power flow angle, which indicates the angle between the group and phase wave velocities, has lower values for all directions, and this is valid for all phases.

The phonon dispersion curves could be used to determine the dynamic stability of a compound. The phonon dispersion curves and phonon density of states are obtained for TiVFeZ compounds. As shown in Fig. 5, there is no imaginary frequency; these compounds have dynamic stability. As a result, there is no soft phonon modes coming from the distortions for these compounds. In addition for the phonon DOS, the Al atoms contribute more to the higher frequencies due to their smaller atomic mass than other atoms in the structure for TiVFeAl. A similar situation could be observed for TiVFeSi, where the Si atoms contribute more to the higher frequencies. However, Ti and V atoms contribute more to the higher frequencies for TiVFeGe. The Ge atom is the heaviest in the compound and contributes more to the lower frequencies. Furthermore, the distance between the acoustic and low frequency optic phonon modes are related to the thermal conductivity and if the low frequency optic phonon modes suppress the acoustic phonon modes, the thermal conductivity will be lower. As can be seen from the phonon dispersion curves, the suppression of the low frequency optic phonon modes to the acoustic phonon modes is high for TiVFeGe and the order of the thermal conductivities is TiVFeGe < TiVFeAl < TiVFeSi.

In addition to the phonon dispersion curves, the thermodynamic properties, including heat capacity, entropy, internal energy, and free energy are obtained for TiVFeZ (Fig. 6) using the quasi-harmonic Debye model [45]. Heat capacity increases rapidly at about 300 K and, then it reaches a constant value called the

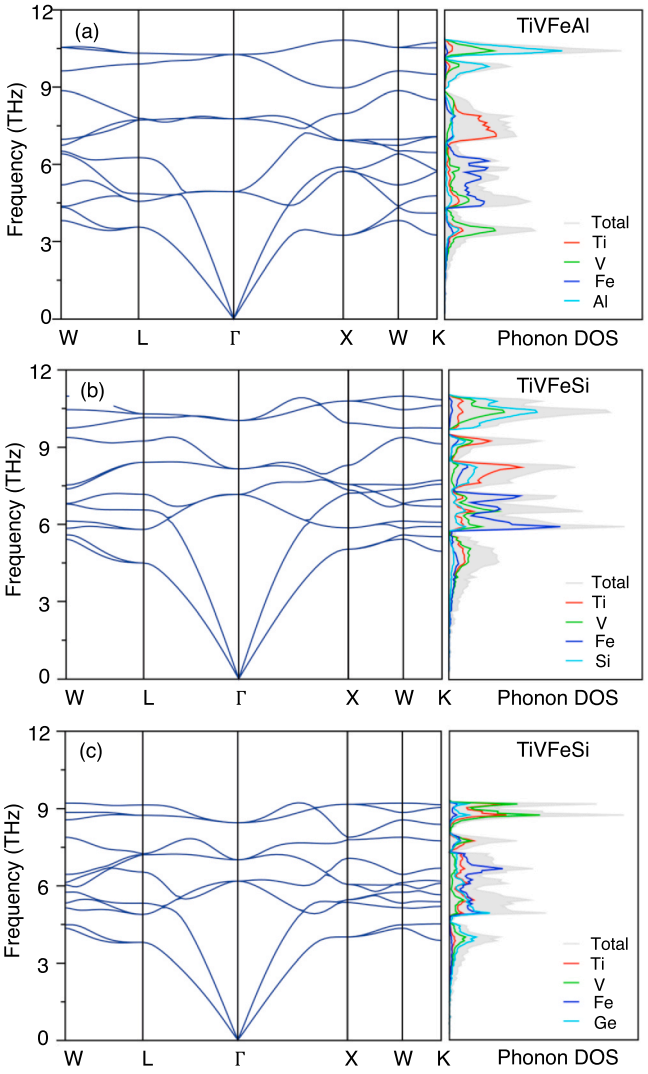

Fig. 5. Phonon dispersion curves with the phonon DOS for (a) TiVFeAl, (b) TiVFeSi and (c) TiVFeGe.

Dulong-Petit limit ($3nR$). All these compounds have similar heat capacities and similar behavior with the temperature increasing. For the entropy, TiVFeGe has the highest value for all the temperature range, and the behavior of the entropy for all the compounds is the same as it increases with the temperature. For the internal energy, TiVFeSi has the lowest value and it increases with the temperature for all compounds. The free energy decreases with the temperature, and TiVFeSi has the highest free energy consistent with lower entropy.

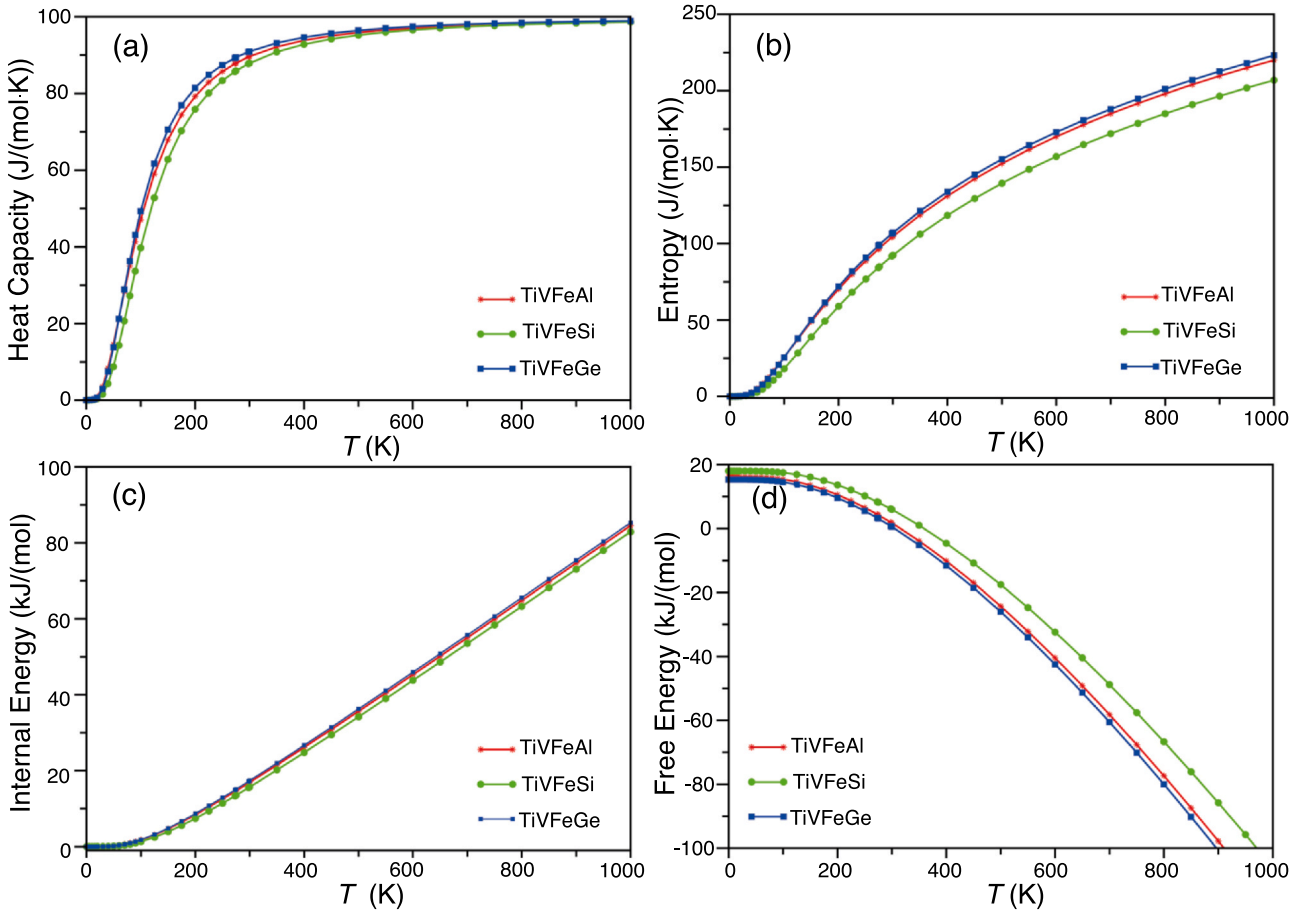

Fig. 6. (a) Heat capacity, (b) entropy, (c) internal energy and (d) free energy for TiVFeZ (Z = Al, Si, Ge) compounds.

4. Conclusion

In this study, TiVFeAl, TiVFeSi, and TiVFeGe EQHCs are identified as potential half-metallic ferromagnetic materials with 488 K, 256 K, and 306 K T_C values respectively. Structural, electronic, magnetic, mechanic, and dynamic properties are analyzed in detail. The γ phase is the most stable phase among the three nonequivalent structures of the TiVFeZ compounds. The calculated elastic constants show that these compounds are mechanically stable. Also, they have dominantly ionic bonding character, and they are ductile materials. The phonon dispersions reveal no imaginary frequencies, indicating dynamic stability. Our work shows that TiVFeAl, TiVFeSi, and TiVFeGe are potential materials for spintronics applications.

CRediT authorship contribution statement

Aysenur Gencer: Data curation, Investigation, Writing - original draft. **Ozge Surucu:** Conceptualization, Investigation, Writing - original draft. **Demet Usanmaz:** Formal analysis, Investigation, Writing - review & editing. **Rabah Khenata:** Conceptualization, Writing - review & editing. **Abdullah Candan:** Data curation, Visualization, Methodology. **Gokhan Surucu:** Methodology, Formal analysis, Validation, Writing - review & editing.

Declaration of Competing Interest

The authors declare that they have no known competing financial interests or personal relationships that could have appeared to influence the work reported in this paper.

Acknowledgements

The calculations were fully performed at TUBITAK ULAKBIM, High Performance and Grid Computing Center (TRUBA resources).

Appendix A. Supporting information

Supplementary data associated with this article can be found in the online version at doi:10.1016/j.jallcom.2021.160869.

References

[1] J.K. Furdyna, N. Samarth, Magnetic properties of diluted magnetic semiconductors: a review (invited), J. Appl. Phys. 61 (1987) 3526–3531, https://doi.org/10.1063/1.338714
[2] J. Xie, First-principles study on the magnetism in ZnS-based diluted magnetic semiconductors, J. Magn. Magn. Mater. 322 (2010) L37–L41, https://doi.org/10.1016/j.jmmm.2010.04.031
[3] A. Roldan, D. Santos-Carballal, N.H. De Leeuw, A comparative DFT study of the mechanical and electronic properties of greigite Fe3S4 and magnetite Fe3O4, J. Chem. Phys. 138 (2013) 204712, https://doi.org/10.1063/1.4807614
[4] K. Schwarz, CrO2 predicted as a half-metallic ferromagnet, J. Phys. F 16 (1986) L211–L215, https://doi.org/10.1088/0305-4608/16/9/002
[5] S. Berri, First-principles study on half-metallic properties of the Sr2GdReO6 double perovskite, J. Magn. Magn. Mater. 385 (2015) 124–128, https://doi.org/10.1016/j.jmmm.2015.03.025
[6] O. Amrich, M. El Amine Monir, H. Baltach, S. Bin Omran, X.W. Sun, X. Wang, Y. Al-Douri, A. Bouhemadou, R. Khenata, Half-Metallic Ferrimagnetic Characteristics of Co2YZ (Z = P, As, Sb, and Bi) New Full-Heusler Alloys: a DFT Study, J. Supercond. Nov. Magn. 31 (2018) 241–250, https://doi.org/10.1007/s10948-017-4206-2
[7] A. Hirohata, K. Yamada, Y. Nakatani, L. Prejbeanu, B. Diény, P. Pirro, B. Hillebrands, Review on spintronics: principles and device applications, J. Magn. Magn. Mater. 509 (2020) 166711, https://doi.org/10.1016/j.jmmm.2020.166711

[8] D.M. Hoat, Investigation on new equiatomic quaternary Heusler compound CoCrIrSi via FP-LAPW calculations, Chem. Phys. 523 (2019) 130–137, https://doi.org/10.1016/j.chemphys.2019.04.009

[9] D.M. Hoat, M. Naseri, Examining the half-metallicity and thermoelectric properties of new equiatomic quaternary Heusler compound CoVRhGe under pressure, Physica B 583 (2020) 412058, https://doi.org/10.1016/j.physb.2020.412058

[10] S. Chatterjee, S. Das, S. Pramanick, S. Chatterjee, S. Giri, A. Banerjee, S. Majumdar, Anomalous transport and magnetic behaviours of the quaternary Heusler compounds CoFeTiSn and CoFeVGa, J. Magn. Magn. Mater. 478 (2019) 155–160, https://doi.org/10.1016/j.jmmm.2019.01.100

[11] J. Drews, U. Eberz, H.U. Schuster, Optische Untersuchungen an farbigen Intermetallischen phasen, J. Less-Common Met. 116 (1986) 271–278, https://doi.org/10.1016/0022-5088(86)90235-3

[12] K. Özdoğan, E. Şaşioğlu, I. Galanakis, Slater-Pauling behavior in LiMgPdSn-type multifunctional quaternary Heusler materials: half-metallicity, spin-gapless and magnetic semiconductors, J. Appl. Phys. 113 (2013) 193903, https://doi.org/10.1063/1.4805063

[13] J. Ji, Q. Gu, R. Khenata, F. Guo, Y. Wang, T. Yang, X. Tan, Structural configuration and tetragonal phase stability in the equiatomic quaternary Heusler compound TiZnMnSi, RSC Adv. 10 (2020) 39731–39738, https://doi.org/10.1039/d0ra07652j

[14] D. Rani, L. Bainsla, K.G. Suresh, A. Alam, Experimental and theoretical investigation on the possible half-metallic behaviour of equiatomic quaternary Heusler alloys: CoRuMnGe and CoRuVZ (Z = Al, Ga), J. Magn. Magn. Mater. 492 (2019) 165662, https://doi.org/10.1016/j.jmmm.2019.165662

[15] Enamullah, Y. Venkateswara, S. Gupta, M.R. Varma, P. Singh, K.G. Suresh, A. Alam, Electronic structure, magnetism, and antisite disorder in CoFeCrGe and CoMnCrAl quaternary Heusler alloys, Phys. Rev. B 92 (2015) 224413, https://doi.org/10.1103/PhysRevB.92.224413

[16] L. Bainsla, A.K. Yadav, Y. Venkateswara, S.N. Jha, D. Bhattacharyya, K.G. Suresh, Local structure studies of CoFeMnX (X = Si and Ge) Heusler alloys using X-ray absorption spectroscopy, J. Alloy. Compd. 651 (2015) 509–513, https://doi.org/10.1016/j.jallcom.2015.08.131

[17] S.A. Khandy, J. Da Chai, Thermoelectric properties, phonon, and mechanical stability of new half-metallic quaternary Heusler alloys: FeRhCrZ (Z = Si and Ge), J. Appl. Phys. 127 (2020) 165102, https://doi.org/10.1063/1.5139072

[18] B. Shi, J. Li, C. Zhang, W. Zhai, S. Jiang, W. Wang, D. Chen, Y. Yan, G. Zhang, P.F. Liu, First-principles investigation on the transport properties of quaternary CoFeRGa (R = Ti, V, Cr, Mn, Cu, and Nb) Heusler compounds, Phys. Chem. Chem. Phys. 22 (2020) 23185–23194, https://doi.org/10.1039/d0cp03226c

[19] Y. Venkateswara, S.S. Samatham, P.D. Babu, K.G. Suresh, A. Alam, Coexistence of spin semimetal and Weyl semimetal behavior in FeRhCrGe, Phys. Rev. B 100 (2019) 180404, https://doi.org/10.1103/PhysRevB.100.180404

[20] O. Cheref, S. Benalia, N. Bettahar, D. Rached, M. Rabah, M. Merabet, L. Djoudi, Insight view of topological nontrivial nature in the novel alkali metal–based quaternary heusler compounds via ab initio calculations, J. Supercond. Nov. Magn. 33 (2020) 3875–3881, https://doi.org/10.1007/s10948-020-05621-z

[21] H.S. Goripati, T. Furubayashi, Y.K. Takahashi, K. Hono, Current-perpendicular-to-plane giant magnetoresistance using Co2Fe(Ga1−xGex) Heusler alloy, J. Appl. Phys. 113 (2013) 043901, https://doi.org/10.1063/1.4788672

[22] L. Bainsla, M.M. Raja, A.K. Nigam, K.G. Suresh, CoRuFeX (X = Si and Ge) Heusler alloys: High TC materials for spintronic applications, J. Alloy. Compd. 651 (2015) 631–635, https://doi.org/10.1016/j.jallcom.2015.08.150

[23] V. Alijani, S. Ouardi, G.H. Fecher, J. Winterlik, S.S. Naghavi, X. Kozina, G. Stryganyuk, C. Felser, E. Ikenaga, Y. Yamashita, S. Ueda, K. Kobayashi, Electronic, structural, and magnetic properties of the half-metallic ferromagnetic quaternary Heusler compounds CoFeMnZ (Z=Al, Ga, Si, Ge), Phys. Rev. B 84 (2011) 224416, https://doi.org/10.1103/PhysRevB.84.224416

[24] L. Xiong, L. Yi, G.Y. Gao, Search for half-metallic magnets with large half-metallic gaps in the quaternary Heusler alloys CoFeTiZ and CoFeVZ (Z=Al, Ga, Si, Ge, As, Sb), J. Magn. Magn. Mater. 360 (2014) 98–103, https://doi.org/10.1016/j.jmmm.2014.02.050

[25] Y.J. Zhang, Z.H. Liu, G.T. Li, X.Q. Ma, G.D. Liu, Magnetism, band gap and stability of half-metallic property for the quaternary Heusler alloys CoFeTiZ (Z = Si, Ge, Sn), J. Alloy. Compd. 616 (2014) 449–453, https://doi.org/10.1016/j.jallcom.2014.07.165

[26] X. Dai, G. Liu, G.H. Fecher, C. Felser, Y. Li, H. Liu, New quarternary half metallic material CoFeMnSi, J. Appl. Phys. 105 (2009) 07E901, https://doi.org/10.1063/1.3062812

[27] G. Kresse, J. Furthmüller, Efficiency of ab-initio total energy calculations for metals and semiconductors using a plane-wave basis set, Comput. Mater. Sci. 6 (1996) 15–50, https://doi.org/10.1016/0927-0256(96)00008-0

[28] G. Kresse, J. Furthmüller, Efficient iterative schemes for ab initio total-energy calculations using a plane-wave basis set, Phys. Rev. B - Condens. Matter Mater. Phys. 54 (1996) 11169–11186, https://doi.org/10.1103/PhysRevB.54.11169

[29] J.P. Perdew, K. Burke, M. Ernzerhof, Generalized gradient approximation made simple, Phys. Rev. Lett. 77 (1996) 3865–3868, https://doi.org/10.1103/PhysRevLett.77.3865

[30] P.E. Blöchl, Projector augmented-wave method, Phys. Rev. B. 50 (1994) 17953–17979, https://doi.org/10.1103/PhysRevB.50.17953

[31] D. Joubert, From ultrasoft pseudopotentials to the projector augmented-wave method, Phys. Rev. B - Condens. Matter Mater. Phys. 59 (1999) 1758–1775, https://doi.org/10.1103/PhysRevB.59.1758

[32] J.D. Pack, H.J. Monkhorst, "special points for Brillouin-zone integrations"-a reply, Phys. Rev. B 16 (1977) 1748–1749, https://doi.org/10.1103/PhysRevB.16.1748

[33] Y. Le Page, P. Saxe, Symmetry-general least-squares extraction of elastic data for strained materials from ab initio calculations of stress, Phys. Rev. B - Condens. Matter Mater. Phys. 65 (2002) 1–14, https://doi.org/10.1103/PhysRevB.65.104104

[34] W. Tang, E. Sanville, G. Henkelman, A grid-based Bader analysis algorithm without lattice bias, J. Phys. Condens. Matter 21 (2009) 084204, https://doi.org/10.1088/0953-8984/21/8/084204

[35] PHONON Software, (n.d.). ⟨http://www.computingformaterials.com/index.html⟩ (Accessed June 18, 2021).

[36] K. Parlinski, Z.Q. Li, Y. Kawazoe, First-principles determination of the soft mode in cubic ZrO2, Phys. Rev. Lett. 78 (1997) 4063–4066, https://doi.org/10.1103/PhysRevLett.78.4063

[37] S. Steiner, S. Khmelevskyi, M. Marsmann, G. Kresse, Calculation of the magnetic anisotropy with projected-augmented-wave methodology and the case study of disorderedFe1−xCoxalloys, Phys. Rev. B 93 (2016) 224425, https://doi.org/10.1103/PhysRevB.93.224425

[38] G. Surucu, B. Yildiz, A. Erkisi, X. Wang, O. Surucu, The investigation of electronic, anisotropic elastic and lattice dynamical properties of MAB phase nanolaminated ternary borides: M2AlB2 (M=Mn, Fe and Co) under spin effects, J. Alloy. Compd. 838 (2020) 155436, https://doi.org/10.1016/j.jallcom.2020.155436

[39] H.L. Huang, J.C. Tung, H.T. Jeng, A first-principles study of rare earth quaternary Heusler compounds: RXVZ (R = Yb, Lu; X = Fe, Co, Ni; Z = Al, Si), Phys. Chem. Chem. Phys. 23 (2021) 2264–2274, https://doi.org/10.1039/d0cp05191h

[40] M. Born, On the stability of crystal lattices. I, Math. Proc. Camb. Philos. Soc. 36 (1940) 160–172, https://doi.org/10.1017/S0305004100017138

[41] A. Gencer, G. Surucu, Electronic and lattice dynamical properties of Ti2SiB MAX phase, Mater. Res. Express 5 (2018) 076303, https://doi.org/10.1088/2053-1591/aace7f

[42] A. Gencer, O. Surucu, G. Surucu, E. Deligoz, Anisotropic mechanical properties of Tl4Ag18Te11 compound with low thermal conductivity, J. Solid State Chem. 289 (2020) 121469, https://doi.org/10.1016/j.jssc.2020.121469

[43] J.W. Jaeken, S. Cottenier, Solving the Christoffel equation: Phase and group velocities, Comput. Phys. Commun. 207 (2016) 445–451, https://doi.org/10.1016/j.cpc.2016.06.014

[44] F.I. Fedorov, General equations of the theory of elasticity, Theory Elastic Waves Cryst, Springer, US, 1968, pp. 1–33, https://doi.org/10.1007/978-1-4757-1275-9_1

[45] A. Togo, I. Tanaka, First principles phonon calculations in materials science, Scr. Mater. 108 (2015) 1–5, https://doi.org/10.1016/j.scriptamat.2015.07.021